Cell Reports, Volume *36*

Supplemental information

Microglial lysosome dysfunction contributes to white matter pathology and TDP-43 proteinopathy in *GRN*-associated FTD

Yanwei Wu, Wei Shao, Tiffany W. Todd, Jimei Tong, Mei Yue, Shunsuke Koga, Monica Castanedes-Casey, Ariston L. Librero, Chris W. Lee, Ian R. Mackenzie, Dennis W. Dickson, Yong-Jie Zhang, Leonard Petrucelli, and Mercedes Prudencio

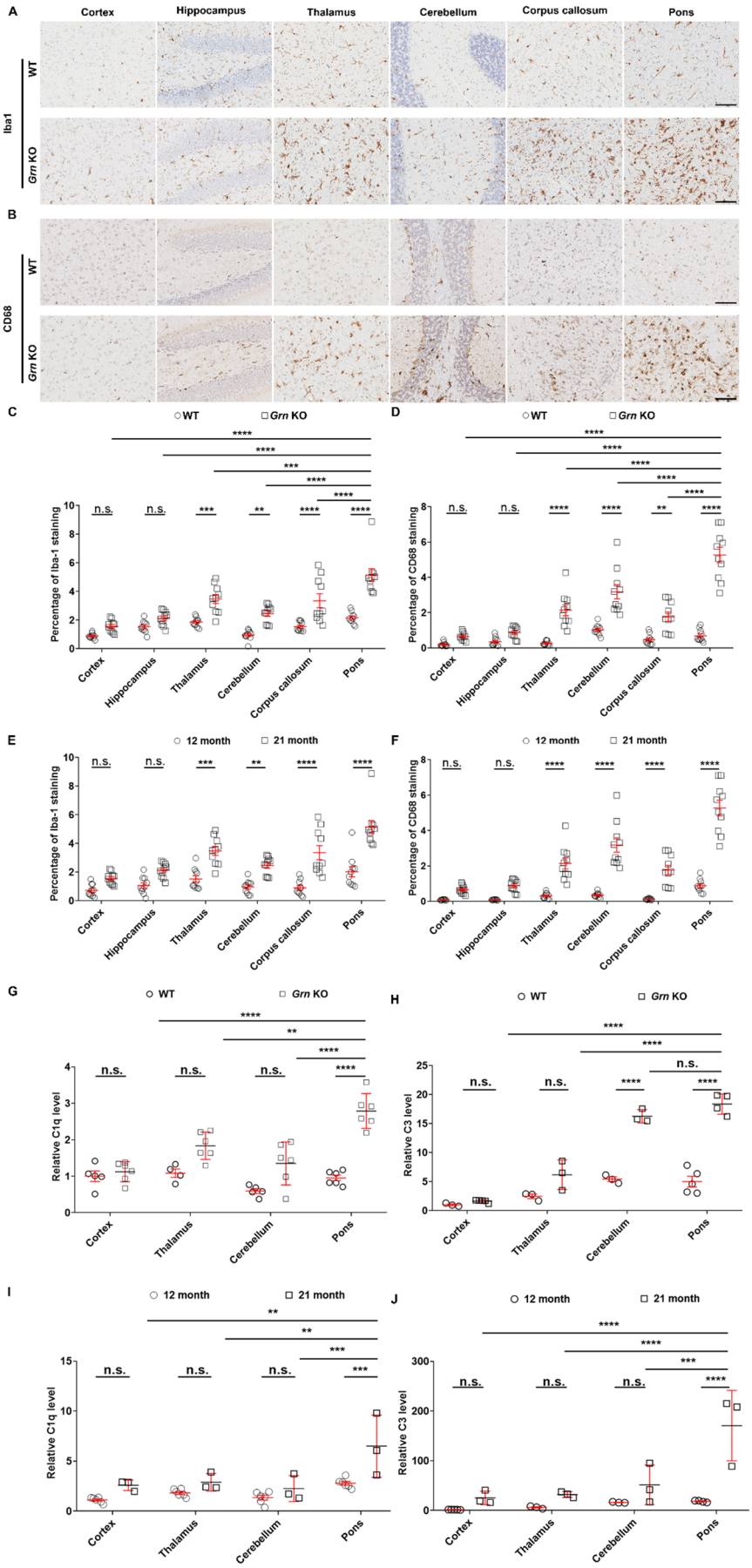
A
Cortex
Hippocampus
Thalamus
Cerebellum
Corpus callosum
Pons
Iba1
WT
Grn KO
B
CD68
WT
Grn KO
C
WT
Grn KO
Percentage of Iba-1 staining
n.s.
n.s.
***
**
****
****
Cortex
Hippocampus
Thalamus
Cerebellum
Corpus callosum
Pons
D
WT
Grn KO
Percentage of CD68 staining
n.s.
n.s.
****
****
**
****
Cortex
Hippocampus
Thalamus
Cerebellum
Corpus callosum
Pons
E
12 month
21 month
Percentage of Iba-1 staining
n.s.
n.s.
***
**
****
****
Cortex
Hippocampus
Thalamus
Cerebellum
Corpus callosum
Pons
F
12 month
21 month
Percentage of CD68 staining
n.s.
n.s.
****
****
****
****
Cortex
Hippocampus
Thalamus
Cerebellum
Corpus callosum
Pons
G
WT
Grn KO
Relative C1q level
n.s.
n.s.
n.s.
****
**
****
****
Cortex
Thalamus
Cerebellum
Pons
H
WT
Grn KO
Relative C3 level
n.s.
n.s.
****
n.s.
****
****
****
Cortex
Thalamus
Cerebellum
Pons
I
12 month
21 month
Relative C1q level
n.s.
n.s.
n.s.
**
**
***
***
Cortex
Thalamus
Cerebellum
Pons
J
12 month
21 month
Relative C3 level
n.s.
n.s.
n.s.
****
****
***
****
Cortex
Thalamus
Cerebellum
Pons

Figure S1. An age-dependent increase in microglial activation is observed in white matter regions of *Grn* KO mice. Related to Figure 1. (**A**-**F**) Representative images (**A**, **B**) and quantitative analyses (**C-F**) of Iba1 (**A**, **C**, **E**) and CD68 (**B**, **D**, **F**) staining in different brain regions of 21-month-old (**A-F**) and 12-month old (**E**, **F**) wild-type (WT) and *Grn* KO mice (n = 10 per group). Scale bar, 50 μm. (**G**-**J**) Quantitative RT-PCR analyses of C1q (**G**, **I**) and C3b (**H**, **J**) RNA levels in different brain regions of 21-month-old (**G**-**J**) and 12-month-old (**I, J**) wild-type (WT) and *Grn* KO mice (n = 3-6 per group). Data are presented as mean ± S.E.M. $^{**}P < 0.01$, $^{***}P < 0.001$, $^{****}P < 0.0001$, 2-way ANOVA, Tukey's multiple-comparison test. n.s.: not significant.

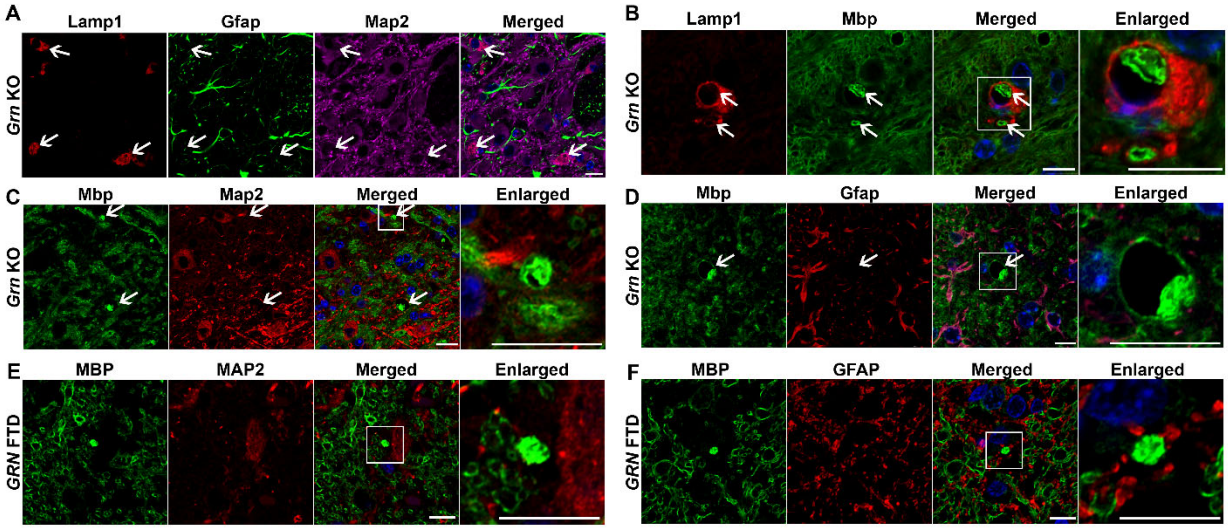

Figure S2. Mbp-positive myelin deposits accumulate in microglial lysosomes in *Grn* KO mice and cases with *GRN* FTD. Related to Figures 1 and 2. (**A**, **B**) Representative images of the pons of 21-month-old *Grn* KO mice co-stained for lysosome (Lamp1) and astrocyte (Gfap) and neuron (Map2) markers (**A**), and lysosome (Lamp1) and oligodendrocyte (Mbp) markers (**B**). Arrows indicate enlarged lysosomes. (**C**, **D**) Representative images of myelin (Mbp) and neuron marker (Map2) (**C**), and myelin (Mbp) and astrocyte marker (Gfap) (**D**) co-staining in the pons of 21-month-old *Grn* KO mice. Arrows indicate myelin debris. (**E, F**) Representative images of myelin (MBP) and neuron marker (MAP2) (**E**), and myelin (MBP) and astrocyte marker (GFAP) (**F**) in the pons of *GRN* FTD. Boxes in B-F indicate the region enlarged in the enlarged panel. Scale bar, 10 μm.

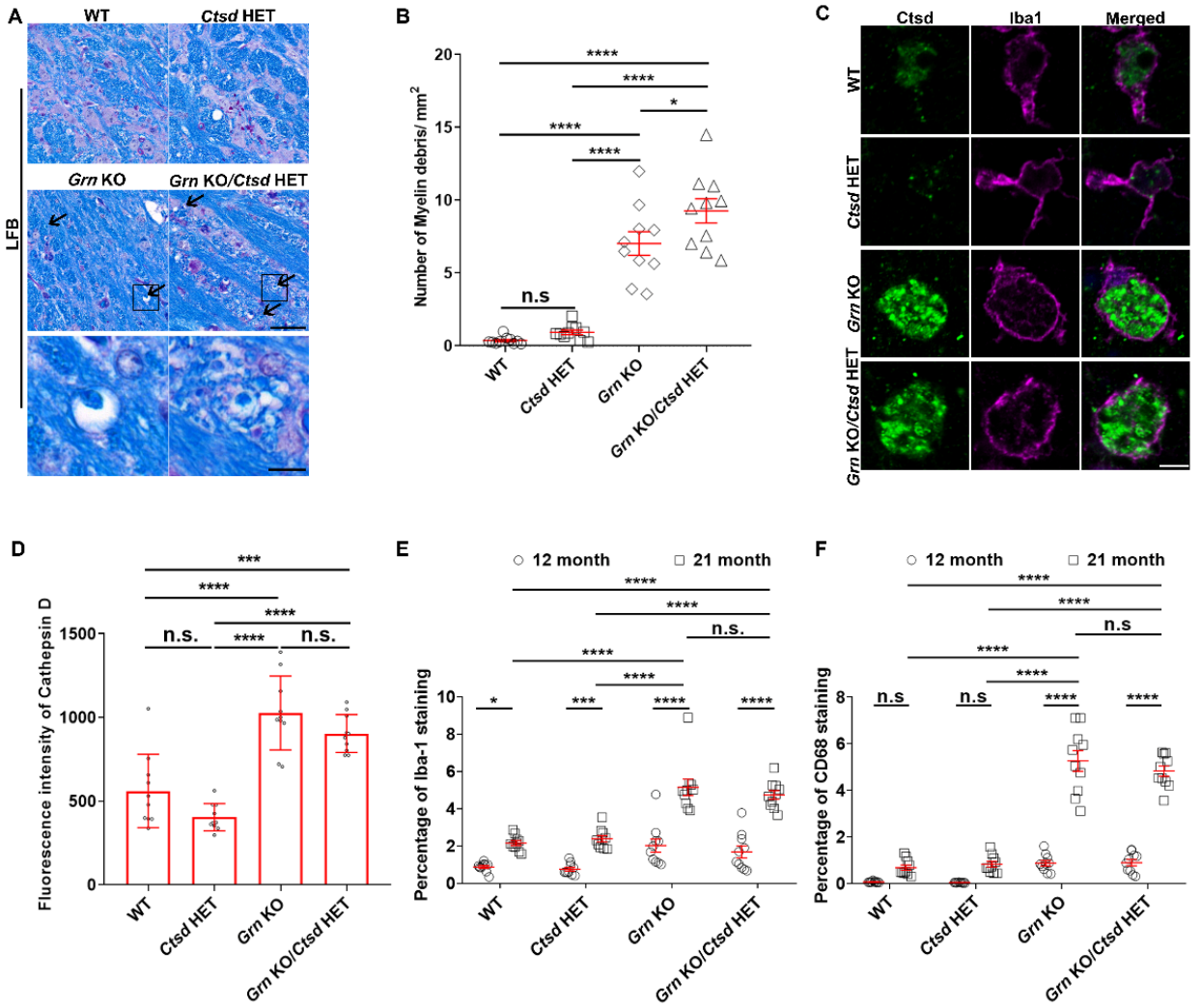

Figure S3. The accumulation of myelin debris, but not microgliosis, in *Grn* KO mice is further enhanced by partial loss of Ctsd. Related to Figure 3. (**A, B**) Representative images (**A**) and quantitative analysis (**B**) of myelin staining (LFB) in the pons of 21-month-old WT, *Ctsd* HET, *Grn* KO or *Grn* KO/*Ctsd* HET mice (n = 10 per group). Arrows indicate myelin debris. Boxes in **A** indicate the region enlarged below. (**C, D**) Representative images (**C**) and quantitative analysis (**D**) of microglia Ctsd staining in the pons of 21-month-old WT, *Ctsd* HET, *Grn* KO or *Grn* KO/*Ctsd* HET mice (n = 10 per group). (**E, F**) Quantitative analysis of Iba1 (**E**) and CD68 (**F**) staining in the pons of 12- and 21-month-old WT, *Ctsd* HET, *Grn* KO or *Grn* KO/*Ctsd* HET mice (n = 10 per group). Scale bar, 50 μm (**A**), and 10 μm (**C**). All data are presented as mean ± S.E.M. *$P < 0.05$, ***$P < 0.001$, ****$P < 0.0001$, 2-way ANOVA, Tukey's multiple-comparison test. n.s.: not significant.

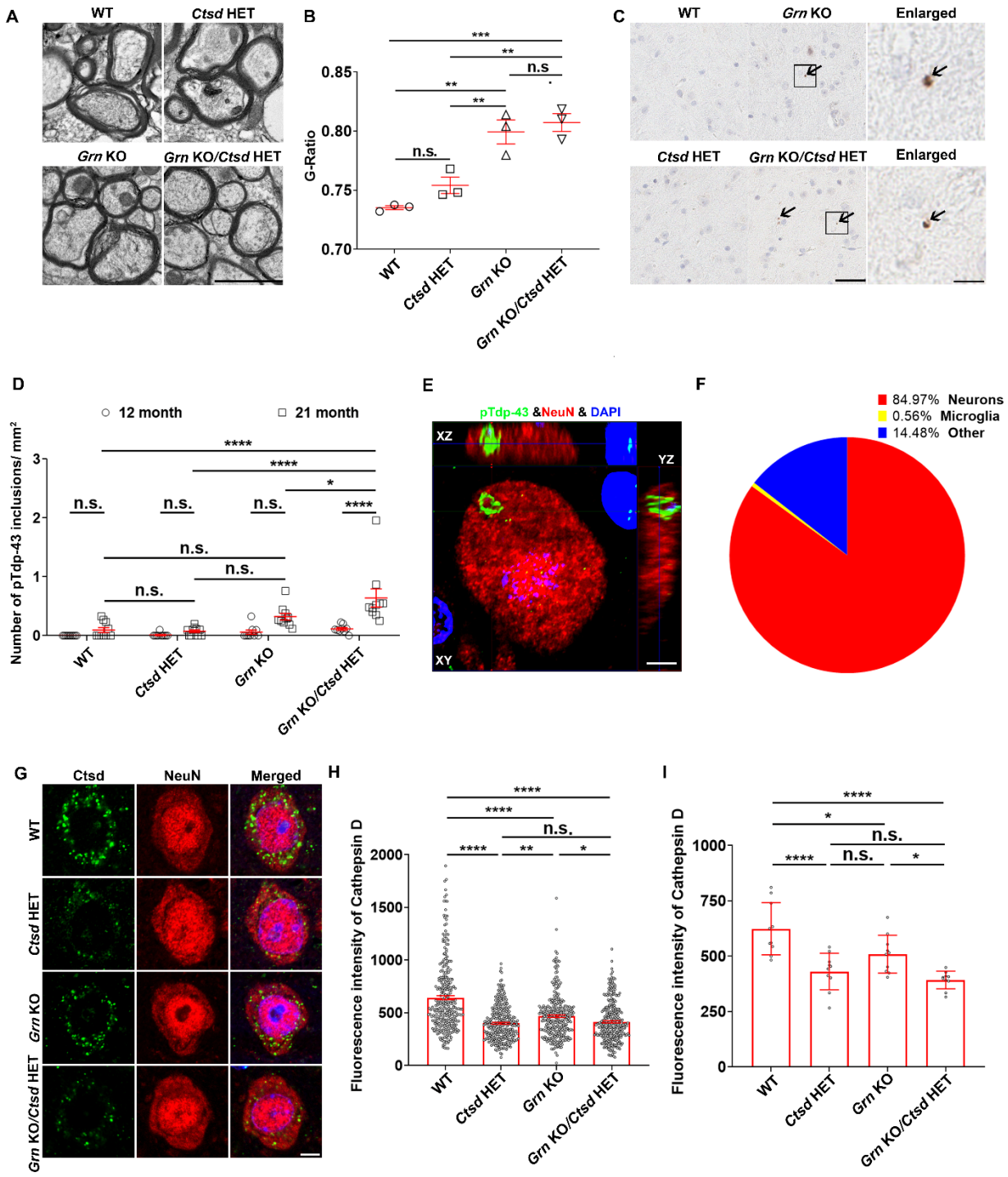

Figure S4. Demyelination and pTdp-43 inclusions are observed in *Grn* KO and Grn KO/Ctsd HET mice. Related to Figure 4. (**A, B**) Representative images (**A**) and quantitative analysis of G-ratio (**B**) of myelinated axons in pons of 12-month-old WT, *Ctsd* HET, *Grn* KO and *Grn* KO/*Ctsd* HET mice (n= 3 per group). (**C** and **D**) Representative images (**C**) in the thalamus of 21-month-old *Grn* KO mice and quantitative analysis (**D**) of pTdp-43 staining in the same region of 12- and 21-month-old WT, *Ctsd* HET, *Grn* KO or *Grn* KO/*Ctsd* HET mice (n = 10 per

group). (**E**) Z-stack confocal image of pTdp-43 and NeuN co-staining in pons of a representative 21-month-old *Grn* KO mouse. (**F**) Quantification analysis of percentage of pTdp-43 in different cell types (n=10). (**G-I**) Representative images (**G**) and quantitative analyses (**H, I**) of neuronal Ctsd staining in the pons of 21-month-old WT, *Ctsd* HET, *Grn* KO or *Grn* KO/*Ctsd* HET mice (n = 300 cells per group for **H**, n= 10 mice per group for **I**). Scale bar, 2 μm (**A**), 5 μm (**E**), 10 μm (**G**) and 50 μm (**C**). Data in graphs is presented as mean ± S.E.M. Statistical differences result from a 2-way ANOVA (**D**) or one-way ANOVA (**B, H, I**), followed by Tukey's multiple-comparison test. *$P < 0.05$, **$P < 0.01$, ***$P < 0.001$, ****$P < 0.0001$, n.s.: not significant

Table S1. Clinical characteristics associated with the samples from patients with FTD used in this study. Related to Figure 2.

Case #	Sex	Age at onset (yrs)	Disease duration (yrs)	*Grn* gene status
1	Male	77	10	Negative
2	Male	61	3	Negative
3	Male	70	11	Negative
4	Male	61	3	Negative
5	Male	67	1	Negative
6	Female	88	N/A	Negative
7	Female	81	3	Negative
8	Male	70	7	Negative
9	Female	73	10	Positive
10	Male	72	10	Positive
11	Male	60	6	Positive
12	Female	69	6	Positive
13	Male	63	5	Positive
14	Female	67	3	Positive
15	Female	71	3	Positive
16	Male	60	10	Positive
17	Male	60	6	Positive

N/A: not available

Table S2. Primary antibodies for immunohistochemistry and immunofluorescence staining. Related to STAR Methods.

Antibody	Species	Dilution	Application	Origin	Catalog number
anti-pTdp-43	rabbit	1:1000	IHC, IF	RB3655: Antibody described in J. Chew et al., Science 348, 1151-1154 (015).	N/A
anti-Iba1	rabbit	1:3000 1:1000	IHC IF	Wako Chemicals	019-19741
anti-CD68	rabbit	1:250 1:500	IHC IF	Abcam	ab125212
anti-Mbp	mouse	1:500	IHC, IF	R&D systems	MAB42282
anti-Lamp1	rat	1:500	IF	Invitrogen	14-1071-82
anti-Map2	mouse	1:500	IF	Sigma	M1406
anti-Gfap	rabbit	1:2000	IF	Biogenex	PU020-UP
anti-Cathepsin D	rabbit	1:500	IF	ProteinTech	21327-1-AP
anti-Ubi1	mouse	1:1000	IF	EMD Millipore	MAB1510
anti-NeuN	mouse	1:1000	IF	Chemicon International	MAB377

IHC: Immunohistochemistry; IF: Immunofluorescence; N/A: not applicable